2013 European Control Conference (ECC)
July 17-19, 2013, Zürich, Switzerland.

I-PD Controller Design based on Generalized KYP Lemma for Ball and Plate System

Shuichi Mochizuki[1] and Hiroyuki Ichihara[2]

Abstract— **A ball-on-plate balancing system, the ball and plate, has a camera to catch a ball position and a plate whose angle of inclination is limited. This paper proposes a design method of PID control based on the generalized Kalman-Yakubovich-Popov lemma for the ball and plate. The design method has two features: the first one is that a structure of the controller is called I-PD to suppress a large input signal against a major change of the reference signal; the second one is that a filter is introduced into the feedback loop to reduce an influence of the noise measurement from the camera. Both simulation and experiment evaluate the effectiveness of the design method.**

I. INTRODUCTION

The ball and plate system [1] demonstrates nonlinear control problems with open-loop unstable and under-actuated. This under-actuated system has four degrees of freedom (DOF) with only two actuators. Thus the four DOF system has to be stabilized by just two control inputs, while motion of the ball is indirectly manipulated by the slopes of the plate [2]. If the plate is not perfectly horizontal, balls go to the edge of the plate and fall down. To stabilize the ball, a control system which measures the position of the ball and adjusts the plate inclination angle are required. The system is two dimensional expansion of the ball and beam [3]. Nowadays the ball and plate system has been controlled by many control methods: PID control [4], fuzzy control [5], neural network control [4], [6], model predictive control [7] and so on.

In positioning and trajectory tracking control of the ball, it is necessary to design feedback controllers such as proportional integral derivative (PID) by considering a limitation of the inclination angle of the plate with better responses. In general, when there is a jump in reference signal, the output of the proportional and the derivative controller may also generate a large input signal, which may saturate the actuator [8]. Considering the above-mentioned problems, this paper designs an optimal controller whose actuator load is low.

This paper proposes a design method of PID control based on the generalized Kalman-Yakubovich-Popov (GKYP) lemma for the ball and plate. As a reason for choosing the PID controller while there are a variety of control methods, the PID controller has the fixed order and robustness. The GKYP lemma is applied to design a feedback control such that the specifications of the open-loop transfer function. Two features of this method are that the structure of the controller is called I-PD (integral-proportional derivative) to suppress a large input signal against a major change of the reference signal, and that a filter is introduced into the feedback loop to reduce the influence of the noise measurement from the camera.

The paper is organized as follows. The ball and plate system and its modeling are described in Section II. The low-pass filter and the I-PD controller based on the GKYP lemma are provided in Section III. The control system is designed in Section IV. The simulation and the experimented results are also presented. Finally, concluding remarks are provided.

The notation used is standard. For a matrix M, its transpose and complex conjugate transpose are denoted by M^T and M^*, respectively. For a Hermitian matrix, $M > (\geq)\, 0$ and $M < (\leq)\, 0$ denote positive (semi)definiteness and negative (semi)definiteness. The symbol $\mathbf{H}_n$ stands for the set of $n \times n$ Hermitian matrices. The subscript n will be omitted if $n = 2$. The real and the imaginary parts of M are denoted by $\Re(M)$ and $\Im(M)$. For matrices Φ and P, $\Phi \otimes P$ means the Kronecker product.

II. BALL AND PLATE SYSTEM

The 2D Ball Balancer is shown in Fig. 1. This ball and plate system made by QUANSER consists of a plate, a ball, an overhead camera and two servo units. The plate is allowed to swivel about any direction. The overhead camera measures the position of the ball. The two servo units underneath the plate are QUANSER SRV02 devices. The SRV02 have a peak time approximately equal to 0.20 seconds, an overshoot approximately equal to 5 percent. Each of them are connected to the side of the plate, by using two DOF gimbals. The sampling time of the system and the frame rate provided by the camera are 1 millisecond and 60 frames per second, respectively. Hence, the image information is

Fig. 1. 2D Ball Balancer

*This work was not supported by any organization.

[1]S. Mochizuki is with the Graduate School of Science and Technology, Meiji University, 1-1-1 Higashimita, Tama-ku, Kawasaki-shi, Kanagawa, 214-8571 Japan ce22062 at meiji.ac.jp

[2]H. Ichihara is with the Department of Science and Engineering, Meiji University, 1-1-1 Higashimita, Tama-ku, Kawasaki-shi, Kanagawa, 214-8571 Japan ichihara at messe.meiji.ac.jp

renewed every about 17 milliseconds. Moreover, the visual system has a constant time delay less than 60 milliseconds.

A. Modeling

The X-direction of the ball and plate system is illustrated in Fig. 2. Assume that the ball is completely symmetric and homogeneous, and no slipping on the plate. Assume also that all frictions are neglected. The plate rotates in the XY-Cartesian coordinates with the origin at the center of plate.

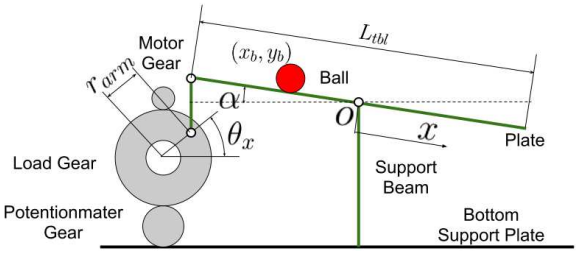

Fig. 2. The ball and plate system

The equations of motion are as follows:

$$\left(m_b + \frac{I_b}{r_b^2}\right)\ddot{x_b} - m_b\left(x_b\dot{\alpha}^2 + y_b\dot{\alpha}\dot{\beta}\right) + m_b g\sin\alpha = 0,$$

$$\left(m_b + \frac{I_b}{r_b^2}\right)\ddot{y_b} - m_b\left(y_b\dot{\beta}^2 + x_b\dot{\alpha}\dot{\beta}\right) + m_b g\sin\beta = 0,$$

where $(x_b,\ y_b)$ is the position of the ball on the plate, α and β are inclination angle of plate to X and Y axis, respectively, m_b is the mass of the ball, r_b is the radius of the ball, g is gravitational acceleration, I_b is the inertia of the ball, L_{tbl} is the side length of the plate, r_{arm} is the length between the joint and the center of the load gear. The numerical values of the constant parameters are shown in Table I. The relationship between α and θ_x is as follows:

$$\sin\alpha = \frac{2\sin\theta_x r_{arm}}{L_{tbl}}. \tag{1}$$

The relationship of β and θ_y is the same as (1) because the both gear system have the same hardware and the plate is symmetrical. When the angular velocity $\dot{\alpha}$ and $\dot{\beta}$ is low, it can be approximated as follows:

$$\dot{\alpha}\dot{\beta} = 0, \quad \dot{\alpha}^2 = 0, \quad \dot{\beta}^2 = 0.$$

Furthermore, by linearizing the motion of equation at $\theta_x = 0$ and $\theta_y = 0$, we get the following equations.

$$\left(m_b + \frac{I_b}{r_b^2}\right)\ddot{x_b} + \frac{2m_b g r_{arm}}{L_{tbl}}\theta_x = 0, \tag{2}$$

TABLE I

PARAMETERS OF THE BALL AND PLATE SYSTEM

Parameters	Numerical values
m_b	0.0252 [kg]
r_b	0.0170 [m]
g	9.81 [m/s^2]
I_b	2.89×10^{-6} [kg·m]
L_{tbl}	0.275 [m]
r_{arm}	0.0254 [m]

$$\left(m_b + \frac{I_b}{r_b^2}\right)\ddot{y_b} + \frac{2m_b g r_{arm}}{L_{tbl}}\theta_y = 0.$$

By linearization the above equations, we can determine two separate differential equations for each of X and Y axis. Here we focus on X axis. Assuming θ_x as input and X_b as output, we find the following transfer function.

$$P(s) = \frac{X_b(s)}{\theta_x(s)} = \frac{K_{bap}}{s^2}, \tag{3}$$

where K_{bap} is

$$K_{bap} = -\frac{2m_b g r_{arm} r_b^2}{L_{tbl}(m_b r_b^2 + I_b)}.$$

Meanwhile, the angles of the load gears θ_x and θ_y are limited as

$$-30\ [^\circ] \le \{\theta_x,\ \theta_y\} \le 30\ [^\circ]. \tag{4}$$

Thus, from (1) the working angles of the plate are

$$-5.3\ [^\circ] \le \{\alpha,\ \beta\} \le 5.3\ [^\circ].$$

B. Measurement noise

There exists inevitably noise from the camera. The FFMV-03M2C-CS made by Point Grey Research, Inc. is a CMOS digital camera, which is used to measure the position of the ball. When the ball keeps still on the plate, steady-state error of the position in the X-axis is shown in the upper part of Fig. 3. The spectral analysis result by using fast Fourier transform is shown in the lower part of Fig. 3. The measurement signals contain a lot of noise at the frequency above 20 [rad/s].

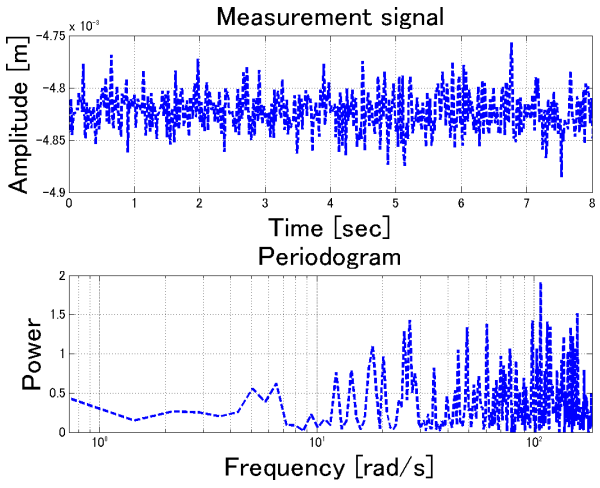

Fig. 3. The measurement signal and periodogram

III. I-PD CONTROL BY GKYP LEMMA

A. First-order low-pass filter

It is necessary to pre-filter the measurement signal before it is fed back. Thus, a filter is introduced into the feedback loop to reduce the influence of the measurement noise [8]. To reduce the high frequency components of the measurement

noise (see Fig. 3), a first-order low-pass filter is designed as follows:

$$F(s) = \frac{a}{s+a}, \tag{5}$$

where a is cut-off frequency.

B. I-PD Controller

In standard PID control a major change in reference signals, generates a large input signal by the proportional and the derivative controller, which may saturate the actuator. Then, it may be desirable to use an inner-loop feedback with the proportional and derivative controller. Such one is called as I-PD controller [8], [9]. Only the integral action acts on the error signal, and the proportional and derivative action act only the measurement output. This paper proposes an open-loop shaping method that realizes desirable frequency response of the closed loop using the GKYP lemma. In Fig. 4, the control input u can be written as follows,

$$u = -K_p y + \frac{K_i}{s}(r-y) - \frac{K_d s}{T_d s + 1} y, \tag{6}$$

where $T_d > 0$ is a parameter to approximate the differentiator by a proper transfer function, K_p is the proportional gain, K_i is the integral gain, K_d is the derivative gain. The open-loop transfer function of a cutaway in the loop at the output of $F(s)$ is given as follows:

$$L(s) = F(s)P(s)K(s),$$

where

$$K(s) = K_p + \frac{K_i}{s} + \frac{K_d s}{T_d s + 1}. \tag{7}$$

Note that the open-loop transfer function of the I-PD structure is the same as that of the standard PID structure.

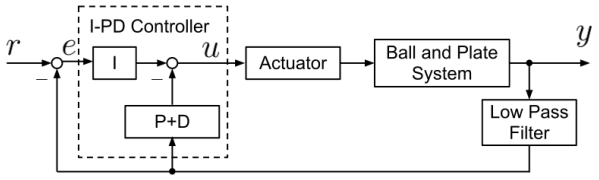

Fig. 4. Diagram of the ball and plate system

C. Generalized KYP lemma

The KYP lemma establishes the equivalence between a frequency domain inequality (FDI) for a transfer function and a linear matrix inequality (LMI) associated with its state-space realization [10]. The standard KYP lemma is applicable for the infinite frequency range while the generalized KYP lemma provides a unified LMI characterization of FDIs in (semi)finite frequency ranges [11]. By introducing the GKYP lemma, design specifications of open-loop transfer function can be result in LMIs.

The frequency range can be represented by

$$\Lambda(\Phi, \Psi) := \{\lambda \in \mathbb{C} \mid \sigma(\lambda, \Phi) = 0,\ \sigma(\lambda, \Psi) \geq 0\} \tag{8}$$

where $\sigma(\lambda, \Phi)$ is defined

$$\sigma(\lambda, \Phi) = \begin{bmatrix}\lambda^* & 1\end{bmatrix} \Phi \begin{bmatrix}\lambda \\ 1\end{bmatrix} = 0$$

for $\lambda \in \mathbb{C}$ and $\Phi,\ \Psi \in \mathbf{H}$. The equality constraint $\sigma(\lambda, \Phi) = 0$ related to Φ in (8) has the role to distinguish the continuous time and discrete time. For example we can set Φ to represent a continuous time system such as

$$\Phi := \begin{bmatrix}0 & 1 \\ 1 & 0\end{bmatrix}.$$

On the other hand, the inequality constraint $\sigma(\lambda, \Psi) \geq 0$ related to Ψ in (8) has the role to set the frequency ranges. Table II summarizes the choices of Φ that lead to specific frequency ranges Ψ where ϖ_l, ϖ_h, ϖ_1 and ϖ_2 are given numbers and $\varpi_c := (1+2)/2$. The desired properties of the frequency response can be represented by

$$\Pi = \begin{bmatrix}\Pi_{11} & \Pi_{12} \\ \Pi_{21} & \Pi_{22}\end{bmatrix} \in \mathbf{H}_{m+p},\quad \Pi_{11} \in \mathbf{H}_p,\quad \Pi \geq 0, \tag{9}$$

where m and p are the numbers of inputs and outputs of $L(\lambda)$. For example, when the half plane under a straight line in the complex plane with a, b and c satisfies (10), Π is expressed as (11).

$$a\Re[L(j\omega)] + b\Im[L(j\omega)] < c, \tag{10}$$

$$\Pi = \begin{bmatrix}0 & a - jb \\ a + jb & -2c\end{bmatrix}. \tag{11}$$

Another example is that the interior of the circle of radius r with center at c is given by

$$|L(j\omega) - c|^2 < r^2, \tag{12}$$

$$\Pi = \begin{bmatrix}1 & -c^* \\ -c & |c|^2 - r^2\end{bmatrix}. \tag{13}$$

For $L(\lambda)$, frequency ranges and characteristics that gives the design specification are discussed in the signal.

TABLE II
FREQUENCY RANGES AND Ψ

Frequency	Ψ	ω
Low	$\begin{bmatrix}0 & -j \\ j & 2\varpi_l\end{bmatrix}$	$\omega \leq \varpi_l$
Middle	$\begin{bmatrix}-1 & j\varpi_c \\ -j\varpi_c & \varpi_1\varpi_2\end{bmatrix}$	$\varpi_1 \leq \omega \leq \varpi_2$
High	$\begin{bmatrix}0 & j \\ -j & -2\varpi_h\end{bmatrix}$	$\varpi_h \leq \omega$

Under these preparations, the generalized KYP Lemma is expressed as follows.

Lemma 1: Generalized KYP lemma [11]
Transfer function $L(\lambda) := C(\lambda I - A)^{-1}B + D$, $\Lambda(\Phi, \Psi)$ and Π are given. Assume that $\det(\lambda I - A) \neq 0,\ \forall \lambda \in \Lambda$ is satisfied the below equation,

$$\sigma(L(\lambda), \Pi) < 0,\ \forall \lambda \in \Lambda(\Phi, \Psi)$$

holds if and only if there exist Hermitian matrices P and Q such that

$$\begin{bmatrix} \Gamma & \begin{bmatrix} B \\ D \end{bmatrix} \Pi_{11} \\ \Pi_{11} \begin{bmatrix} B \\ D \end{bmatrix}^* & -\Pi_{11} \end{bmatrix} < 0, \tag{14}$$

where

$$\Gamma := \begin{bmatrix} A & I \\ C & 0 \end{bmatrix} (\Phi^T \otimes P + \Psi^T \otimes Q) \begin{bmatrix} A & I \\ C & 0 \end{bmatrix}^T + \begin{bmatrix} 0 & B\Pi_{12} \\ \Pi_{12}^* B^T & D\Pi_{12} + \Pi_{12}^* D^T + \Pi_{22} \end{bmatrix}.$$

The equation (14) is linear with respect to B, D, P, Q and Π_{22}. In the case where B and D have affine design parameter, (14) is an LMI.

IV. CONTROL SYSTEM DESIGN

A. Filter design

In (5), we set the frequency a with 18.85 [rad/s] considering the control performance and noise reduction. The spectral analysis results of the signal pass through the filter is shown in Fig. 5. The solid and dotted lines represent the signal after passing through the filter and the raw signal, respectively. From the results in spectral analysis (Fig. 5), we found that the noise at the frequency above 20 [rad/s] has been reduced.

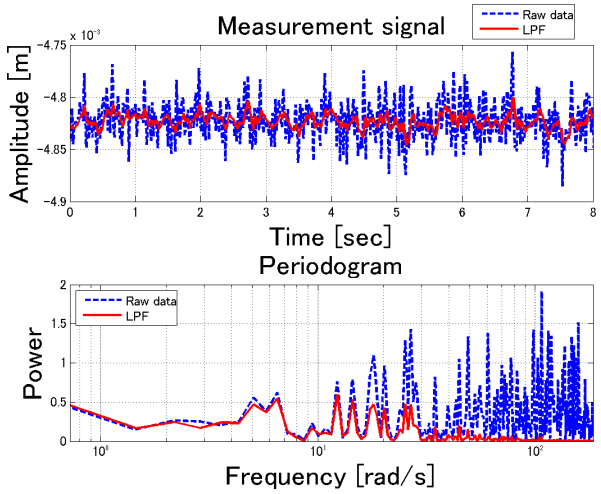

Fig. 5. The measurement signal and periodogram with first-order low-pass filter

B. State-space realization of the open-loop transfer function

To apply the GKYP for the open-loop system, a state-space realization of $L(s)$ is required. For fixed T_d at 0.0001, the design parameters (K_p, K_i, K_d) appear affinely in the numerator of $K(s)$. Indeed, the controllable canonical form of $K(s)$ is expressed as follows,

$$\left[\begin{array}{c|c} A_k & B_k(\rho) \\ \hline C_k & D_k(\rho) \end{array}\right] = \left[\begin{array}{cc|c} 0 & 0 & \frac{K_i}{T_d} \\ 1 & -\frac{1}{T_d} & K_i - \frac{K_d}{T_d^2} \\ \hline 0 & 1 & K_p + \frac{K_d}{T_d} \end{array}\right]. \tag{15}$$

A state-space realization of the ball and plate $P(s)$ is

$$\left[\begin{array}{c|c} A_p & B_p \\ \hline C_p & D_p \end{array}\right] = \left[\begin{array}{cc|c} 0 & 1 & 0 \\ 0 & 0 & K_{bap} \\ \hline 1 & 0 & 0 \end{array}\right]. \tag{16}$$

Similarly, the low-pass filter $F(s)$ can be expressed as

$$\left[\begin{array}{c|c} A_f & B_f \\ \hline C_f & D_f \end{array}\right] = \left[\begin{array}{c|c} -a & 1 \\ \hline a & 0 \end{array}\right]. \tag{17}$$

Combining these realizations (15)-(17), we obtain a realization of the loop transfer function $L(s) := F(s)P(s)K(s)$ as

$$L(s) = \left[\begin{array}{c|c} A & B(\rho) \\ \hline C & D(\rho) \end{array}\right],$$

where

$$A = \begin{bmatrix} A_k & 0 & 0 \\ C_k B_p & A_p & 0 \\ C_k D_p B_f & C_p B_f & A_f \end{bmatrix},$$
$$B = \begin{bmatrix} B_k(\rho) \\ D_k(\rho) B_p \\ D_k(\rho) D_p B_f \end{bmatrix},$$
$$C = \begin{bmatrix} C_k D_p B_f & C_p B_f & C_f \end{bmatrix},$$
$$D = D_k(\rho) D_p D_f.$$

C. The specifications

To shape the Nyquist plot of the open-loop transfer function $L(s)$, we require the following specifications.

$$-0.2\Re[L(j\omega)] + \Im[L(j\omega)] > \gamma_l, \ {}^\forall 0.1 \le \omega \le 0.8 \tag{18}$$
$$\Im[L(j\omega)] < \gamma_m, \ {}^\forall 2.5 \le \omega \le 2.8 \tag{19}$$
$$|L(j\omega)| < \gamma_h, \ {}^\forall \omega \ge 10 \tag{20}$$
$$4\Re[L(j\omega)] + \Im[L(j\omega)] < \gamma_1, \ {}^\forall \omega \ge 0.2 \tag{21}$$
$$4\Re[L(j\omega)] + \Im[L(j\omega)] > \gamma_2, \ {}^\forall \omega \ge 0.2 \tag{22}$$

The spec. (18) with a large $\gamma_l > 0$ ensures sensitivity reduction in the low frequency range by making $L(s)$ high gain. The spec. (19) guarantees a certain stability margin. It is important for the Nyquist plot to be outside of a circle with its center at the point $-1 + j0$. The spec. (20) with small γ_h ensures robustness against unmodelled dynamics which typically exists in the high frequency range. The spec. (21) and (22) are the constraints that adjust the corner angular frequency of the integral action. In the I-PD controller, tracking performance of a reference input depends on the integral action. Here we focus on the minimum value of the frequency interval that can be specified in the spec. (21) and (22). If the minimum value is closer to -90 degrees in the phase diagram of the controller, the integral time T_i is short. On the other hand, if that value is closer to 0 degrees, T_i is long. In other words, T_i is smaller as increasing γ_2. However, it is required to suppress γ_1 which may cause overshoot or hunting if T_i is too small.

D. Design of the I-PD controller

We have designed an I-PD controller by minimizing γ_2 subject to the specs. (18)-(22) where

$$(\gamma_l,\ \gamma_m,\ \gamma_h,\ \gamma_1) = (15,\ -1,\ 0.5,\ 50). \qquad (23)$$

Then, the LMI optimization problem is

$$\begin{aligned} &\text{minimize} && \gamma_2, \\ &\text{subject to} && (18)\text{-}(22),\ (23). \end{aligned}$$

The resulting optimal I-PD controller and optimal value γ_2 are found to be

$$(K_i,\ K_p,\ K_d,\ \gamma_2) = (6.4005,\ 7.8133,\ 3.3631,\ -143.1)$$

by using MATLAB R2011b, YALMIP R20120806 [12] and SPDT3-4 [13]. The nyquist diagram is shown in Fig. 6 and 7, in which $L(j\omega)$ satisfies the design specifications in section IV-C. Since γ_2 is minimized, the low frequency range are closer to the imaginary axis.

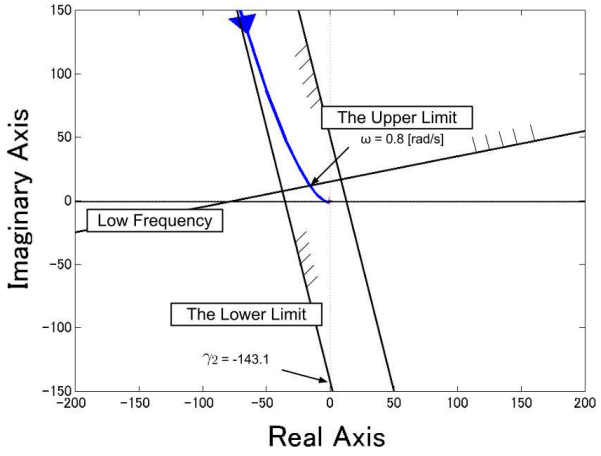

Fig. 6. Nyquist plot

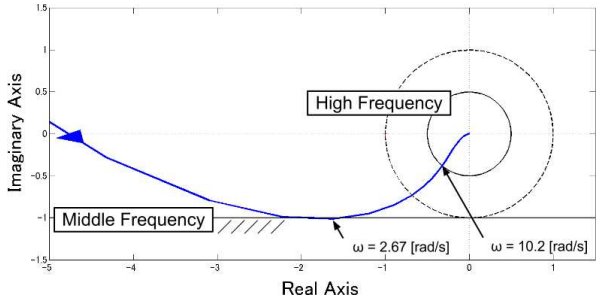

Fig. 7. Nyquist plot (Magnification)

V. SIMULATION RESULTS

The proposed method is verified by comparing the step response of a PID controller and the designed I-PD controller. The both controllers have the same gains. The step response of simulation results is shown in the upper part of Fig. 8. The control inputs in simulation results is shown in the lower part of Fig. 8. From this results, the system input of the I-PD controller satisfies (4), and the response settles down to the desired value without the overshoot. On the other hand, the PID controller does not satisfy the input angle constraint.

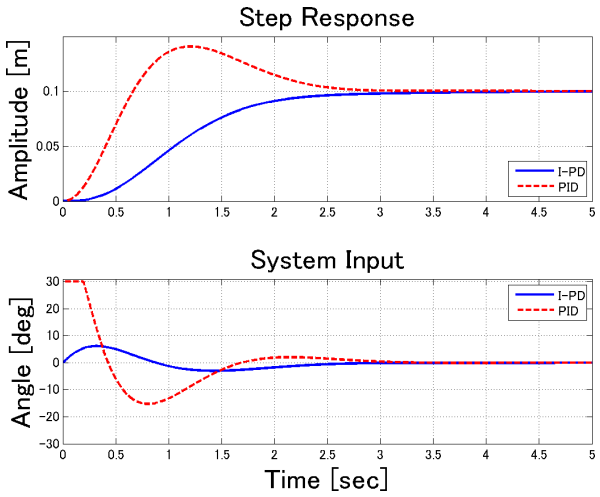

Fig. 8. Simulation results of step response

VI. EXPERIMENTAL RESULTS

A. Experiments of step response control

The proposed I-PD controller design methods using the GKYP lemma for ball and plate system are evaluated with experiments. Experimental conditions are the same as the simulation ones. The results are shown in Fig. 9. Compared with the simulation results, the input is slightly larger, and a delay appears in the response. The cause of the delay are as follows: One is tracking performance of the servo unit. Another is delay on visual feedback system include a frame rate of the camera and image processing. The another is delay introduced by the filter. The rise time and the settling time is almost same as the simulation results.

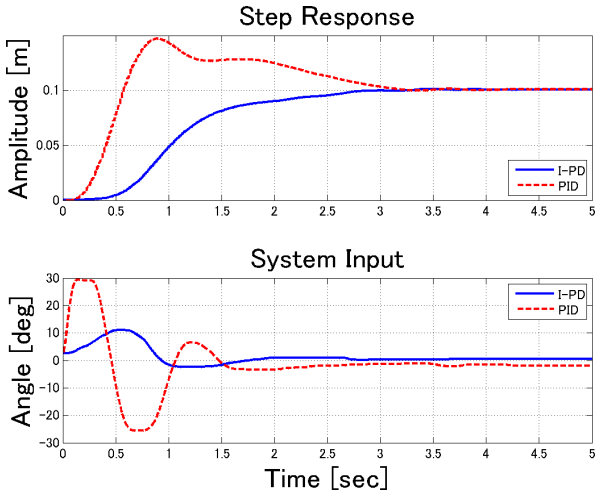

Fig. 9. Experimental results of step response

B. Experiments of trajectory tracking control

The reference trajectories for tracking control are a circle with radius 0.05[m], and a square 0.1[m] on each edge. The trajectories are shown in Fig. 10. The time history of the ball and input angle are shown in Fig. 11 and 12. In the square trajectory control, we obtain similar results as those in the step response. However, focusing on the trajectory (x_b, y_b) of the ball in Fig.11, the response has a slight vibration near the target values. Such vibration phenomena are particularly noticeable in the circular tracking control with control input angle is small. It is suspected that the cause is the friction of the ball against the plate, or the backlash of the gear system.

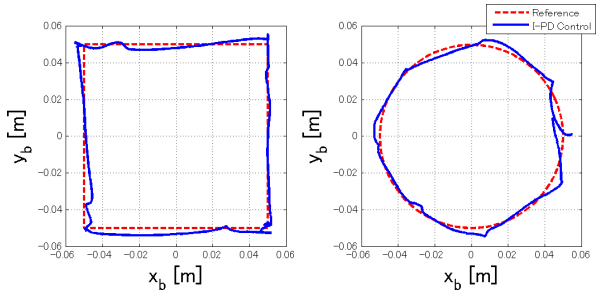

Fig. 10. Experimental results of tracking control

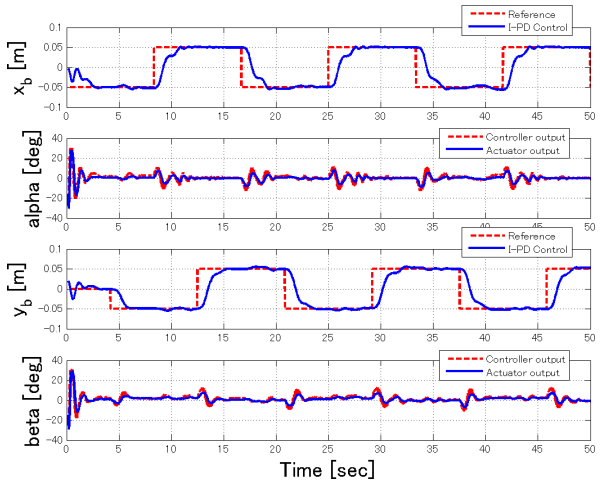

Fig. 11. Experimental results of square response

VII. CONCLUSION

This paper has applied the GKYP lemma to I-PD controller design of the ball and plate system. The multiple specifications on the several frequency ranges have been satisfied by a solution of the LMI optimization problem based on the GKYP lemma. By the first-order low-pass filter, the control performance of the system is improved to reduce the noise in the high frequency range. Both the simulation and experiment have evaluated the effectiveness of the design method. The PI-D (proportional integral-derivative) controller which moved the derivative controller to the inner feedback loop also has the same the open-loop

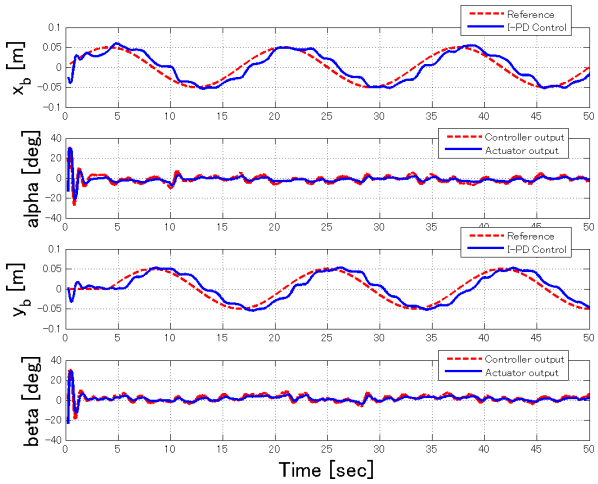

Fig. 12. Experimental results of circle response

transfer function as the standard PID controller. Thus this method can also be applied to the PI-D controller.

ACKNOWLEDGMENT

The authors are very grateful to Bachelor of Engineering, Noor Fatin Binti Hasan belong to Meiji University for her contribution.

REFERENCES

[1] T. Hirochi, M. Yokomichi, and M. Shima, "Control of "Ball and Plate System" by Approximate Input-output Linearization Method," *T. SICE*, vol. 31, no. 10, pp. 1635–1642, 1995.

[2] M. Moarref, S. Mohsen, and G. Vossoughi, "Mechatronic design and position control of a novel ball and plate system," *IEEE Mediterranean Conference on Control and Automation*, pp. 1071–1076, 2008.

[3] P. Kokotovic, "The joy of feedback: nonlinear and adaptive," *IEEE Control Syst. Mag.*, vol. 12, no. 3, pp. 7–17, 1992.

[4] F. Zheng, X. Qian, X. Li, and S. Wang, "Modeling and PID neural network research for the ball and plate system," *International Conference on Electronics Communications and Control*, pp. 331–334, 2011.

[5] F. Xingzhe, Z. Naiyao, and T. Shujie, "Trajectory planning and tracking of ball and plate system using hierarchical fuzzy control scheme," *Fuzzy Sets and Systems*, vol. 144, no. 2, pp. 297–312, Jun. 2004.

[6] M. Bai, Y. Tian, and Y. Wang, "Decoupled Fuzzy Sliding Mode Control to Ball and Plate System," *Intelligent Control and Information*, 2011.

[7] F. Jianchao and H. Min, "Nonliear Model Predictive Control of Ball-Plate System based on Gaussian Particle Swarm Optimization," *IEEE World Congress on Computational Intelligence*, pp. 10–15, 2012.

[8] Q. Li and Z. Kemin, *Introduction to Feedback Control*. Prentice Hall, 2009.

[9] K. J. Åstrőm and T. Hägglund, *ADVANCED PID CONTROL*. Instrumentation Systems, 2005.

[10] A. Rantzer, "On the KalmanYakubovichPopov lemma," *Systems & Control Letters*, vol. 28, pp. 7–10, 1996.

[11] T. Iwasaki and S. Hara, "Generalized KYP Lemma Unified Frequency Domain Inequalities With Design Applications," *IEEE Trans. Autom. Control*, 2005.

[12] J. Lőfberg, "Yalmip : A toolbox for modeling and optimization in MATLAB," in *Proceedings of the CACSD Conference*, Taipei, Taiwan, 2004. [Online]. Available: http://users.isy.liu.se/johanl/yalmip

[13] K. C. Toh, M. Todd, and R. H. Ttnc, "Sdpt3 – a matlab software package for semidefinite programming," *OPTIMIZATION METHODS AND SOFTWARE*, vol. 11, pp. 545–581, 1999.